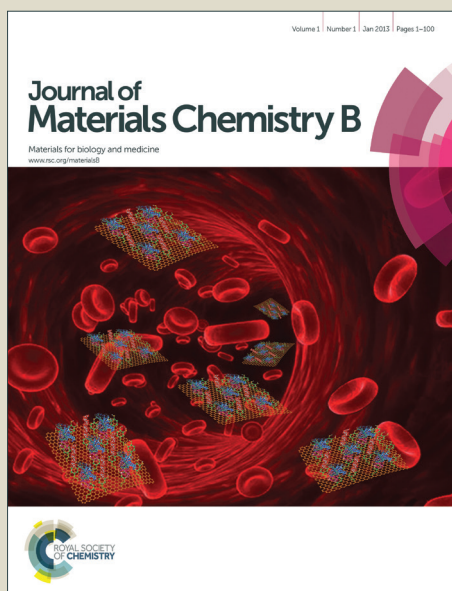


# Journal of Materials Chemistry B

Accepted Manuscript



This is an *Accepted Manuscript*, which has been through the Royal Society of Chemistry peer review process and has been accepted for publication.

*Accepted Manuscripts* are published online shortly after acceptance, before technical editing, formatting and proof reading. Using this free service, authors can make their results available to the community, in citable form, before we publish the edited article. We will replace this *Accepted Manuscript* with the edited and formatted *Advance Article* as soon as it is available.

You can find more information about *Accepted Manuscripts* in the [Information for Authors](#).

Please note that technical editing may introduce minor changes to the text and/or graphics, which may alter content. The journal's standard [Terms & Conditions](#) and the [Ethical guidelines](#) still apply. In no event shall the Royal Society of Chemistry be held responsible for any errors or omissions in this *Accepted Manuscript* or any consequences arising from the use of any information it contains.

**Preparation of PEG-modified PAMAM dendrimers having gold nanorod core  
and their application to photothermal therapy**

Xiaojie Li, Keishi Takeda, Eiji Yuba, Atsushi Harada, Kenji Kono\*

Department of Applied Chemistry, Graduate School of Engineering, Osaka Prefecture  
University

1-1 Gakuen-cho, Naka-ku, Sakai, Osaka 599-8531, Japan.

Tel.: +81 72 254 9330; Fax: +81 72 254 9330; E-mail: kono@chem.osakafu-u.ac.jp.

Running title: PEG-modified dendrimers having gold nanorod core

\*To whom correspondence should be addressed: Department of Applied Chemistry,  
Graduate School of Engineering, Osaka Prefecture University, 1-1 Gakuen-cho,  
Naka-ku, Sakai, Osaka 599-8531, Japan. Tel.: +81 72 254 9330; Fax: +81 72 254  
9330; E-mail: kono@chem.osakafu-u.ac.jp.

**Abstract**

This study was conducted to attempt development of a new type of hybrid dendrimer consisting of a gold nanorod (GNR) core and PEG-modified PAMAM (PEG-PAMAM) dendrons by adding PEG-PAMAM G2-G4 dendrimers with cystamine core at various times during the GNR growing reaction. We obtained 18-25 nm hybrids of the dendrimers and GNR exhibiting surface plasmon resonance in the near infrared region. Whereas PEG-PAMAM G4 dendrimer-GNR hybrid formed aggregate in an aqueous solution, PEG-PAMAM G2 and G3 dendrimers respectively gave hybrids with average diameters of 24 nm and 31 nm. Especially, the spherical PEG-PAMAM G3 dendrimer-GNR hybrid might be regarded as a GNR-core PEG-PAMAM dendrimer in which the GNR core was well stabilized by highly hydrated PEG-PAMAM G3 dendrons. The GNR-core PEG-PAMAM G3 dendrimer exhibited excellent heat-generation capability under near-infrared light irradiation. Incubation with the GNR-core PEG-PAMAM G3 dendrimer showed no damage to HeLa cells. However, dendrimer-treated cells were killed effectively by near-infrared laser irradiation, indicating excellent photothermal capability of the GNR-core PEG-PAMAM G3 dendrimer. Furthermore, GNR-core PEG-PAMAM G3 dendrimer injected into mice tumor tissues significantly increased the temperature of the tumor when irradiated with near infrared light, resulting in decreased tumor volume. These results demonstrate that GNR-core PEG-PAMAM dendrimers might be a new nanomaterial for biomedical applications such as photothermal therapy.

## Introduction

Dendrimers are a family of synthetic polymers with a regularly branched tree-like structure.<sup>1-2</sup> The globular shape given to these dendrimers by such a highly branched backbone provides various surface properties and an interior capable of encapsulating guest materials. Furthermore, because molecular chains of dendrimers are grown stepwise by repeatedly introducing branch structures to their chain ends, their molecular sizes and structures can be controlled precisely. Uniformity at the molecular level and high controllability of the molecular structure and properties make dendrimers highly attractive, especially considering their application to biomedicine, because these dendrimer features might improve the controllability of their behaviors *in vivo*.<sup>3-7</sup>

For application to biomedicine, dendrimers must have bio-related functions to increase their usefulness. Because of the globular structure of dendrimers, the surface region of dendrimers presents particularly attractive moieties for their functionalization.<sup>8-9</sup> Therefore, many studies have been conducted to produce functional dendrimers through surface moiety modification. For example, polyethylene glycol (PEG) chains have been attached to chain terminals of dendrimers to provide a biocompatible surface to dendrimers.<sup>10</sup> In addition, attachment of ligands to dendrimer surface moiety has been used to instill target-specific properties.<sup>11</sup> Temperature-sensitive polymers and their side chain moieties have been conjugated to dendrimer chain terminals to provide temperature-responsive functions to dendrimers.<sup>12-14</sup>

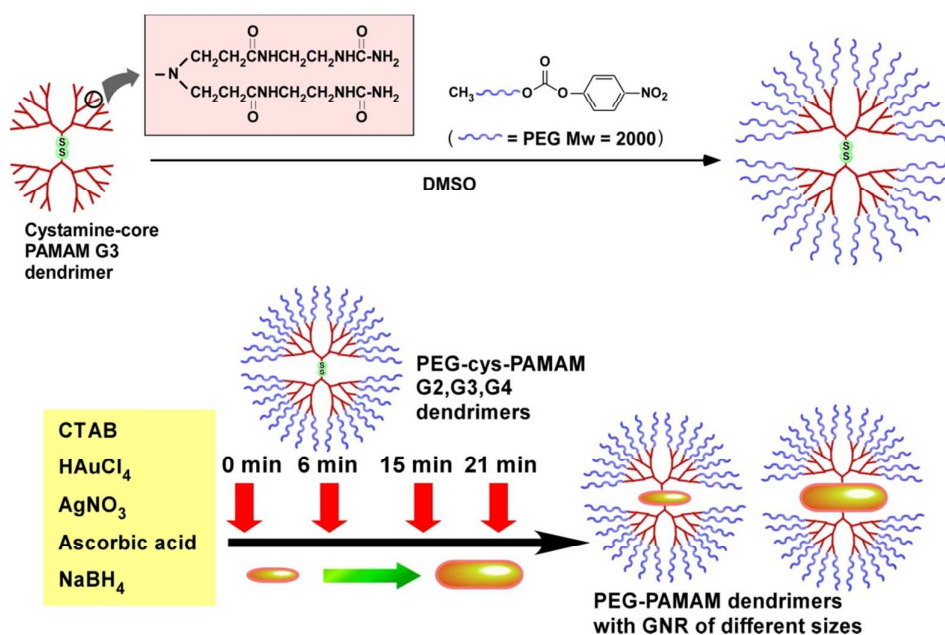
The core moiety of dendrimers might be another site for their functionalization, although few attempts have been made to use this moiety to provide functions to dendrimers. Azobenzene and cystamine residues have been incorporated into the core moiety to create dendrimers with photoresponsive conformational change<sup>15</sup> and reductive environment-responsive cleaving properties<sup>16</sup>, respectively. However, considering their application to biomedicine, the use of metal nanoparticles, especially gold nanoparticles (GNPs), as the core might be of great interest because of their various properties and functions such as photoinduced heat-generating ability, light-emitting property, and radiation-enhancing property, which are applicable to photothermal therapy,<sup>17</sup> bio-imaging,<sup>18-19</sup> X-ray radiation therapy,<sup>20</sup> and so on.<sup>21</sup> In fact, dendrimers having GNPs core have been prepared by reacting GNPs with dendrons of various backbone structures, such as poly(arylether),<sup>22-23</sup> poly(Lys)<sup>24</sup>, and PAMAM<sup>25-26</sup> having reactive groups at the focal point. Such dendrimers with a GNP core might present several important benefits. For example, these AuNP-core dendrimers might have a narrow size distribution derived from uniformity of dendron size. When dendrons have functions such as stimulus-sensitivity, the resultant dendrimers are expected to exhibit multiple functions derived from the GNP core and from dendrimer moieties.

The development of photoactivable nanomaterials has received much attention in recent years for potential biomedical applications in some major areas such as drug and gene delivery, and photodynamic and photothermal therapy.<sup>27</sup> Dendrimers with spherical GNP core have been explored for potential cancer photothermal therapy in

vitro.<sup>17</sup> This therapeutic strategy is based on the conversion of absorbed light energy into heat for hyperthermia using GNP core. However, spherical GNPs exhibit surface plasmon resonance (SPR) with visible light around 530 nm, which has poor ability to penetrate into the body because of absorption by biocomponents including hemoglobin.<sup>28</sup> Near-infrared (NIR, 650-900 nm) light is known to be only minimally absorbed by skin and tissue, which enables deeper tissue penetration up to 10 cm.<sup>28</sup> Therefore, the development of GNP-cored dendrimers having SPR property with NIR light is necessary for effective cancer photothermal therapy applications in vivo. They can release heat inside of the tumors for sufficient tumor ablation by controlling the timing and intensity of NIR light irradiation. For example, gold nanorods (GNRs), gold nanocubes, and gold nanoshells are known to exhibit SPR in the NIR region.<sup>29</sup> Especially, GNRs have been studied intensively for their benefits related to preparation, characteristics, and applications.<sup>30</sup>

It has been demonstrated that the size and aspect ratio of GNRs are affected by methods and conditions for their preparation.<sup>29</sup> However, they are generally larger than dendrimers. Therefore, it is desired to develop synthetic procedure for the preparation of GNRs of dendrimer size for the production of dendrimers having a GNR core. Considering that GNRs were formed by growth from nano-sized seed consisting of Au clusters, we expected that the reaction of dendrimers having Au-reactive groups at the core with growing GNRs might inhibit their further growth by passivating GNR surface, resulting in their hybrids with immature GNRs. For progression to production of GNR-cored dendrimers for biomedical applications, we

synthesized PEG-modified PAMAM dendrimers having a cystamine core for this study. Moreover, we prepared their hybrids by producing GNRs in the presence of the dendrimers with Au-reactive disulfide group. Influence of the dendrimers on the GNP core morphology and their possible application to photothermal therapy were investigated.



Scheme 1. Synthesis of PEG-cys-PAMAM dendrimers and GNR-core PEG-PAMAM dendrimers.

## Experimental Section

### Materials

Gold(III) chloride hydrate ( $\text{HAuCl}_4 \cdot 4\text{H}_2\text{O}$ ), sodium borohydride ( $\text{NaBH}_4$ ), silver nitrate ( $\text{AgNO}_3$ ), and 3-(4,5-dimethyl-2-thiazoryl)-2,5-diphenyl-2H-tetrazolium bromide (MTT) were purchased from Wako Pure Chemical (Osaka, Japan). Cetyltrimethylammonium bromide (CTAB) was obtained from Fluka. PAMAM

dendrimer with cystamine core, generation 2 solution (20 wt. % in methanol), generation 3 solution (10 wt. % in methanol), and generation 4 solution (10 wt. % in methanol); 4-nitrophenyl chloroformate, polyethylene glycol monomethyl ether with the average molecular weight of 2000, and propidium iodide (PI) were obtained from Sigma-Aldrich Japan (Tokyo, Japan). Opti-MEM medium without phenol red and 1,1'-dioctadecyl-3,3,3',3'-tetramethylindocarbocyanine perchlorate (DiI) were obtained from Invitrogen (Carlsbad, USA). Calcein-acetoxymethyl ester (calcein-AM) was from Nacalai Tesque (Kyoto, Japan). PEG (2000) 4-nitrophenyl carbonate (PEG-NPC) was synthesized using 4-nitrophenyl chloroformate and polyethylene glycol monomethyl ether according to our previous report.<sup>10</sup> Tetrahydrofuran (THF), triethylamine (TEA) and dimethyl sulfoxide (DMSO) were supplied from Kishida Chemical (Osaka, Japan), and were distilled just prior to use.

#### ***Synthesis of PEG-PAMAM dendrimers***

PEG-modified cystamine-core PAMAM (PEG-cys-PAMAM) dendrimers were synthesized as reported previously (Scheme 1).<sup>10</sup> A typical synthesis method for PEG-cys-PAMAM G2 dendrimer is as follows: To a solution of cys-PAMAM G2 dendrimer (24.4  $\mu\text{mol}$ ) in dimethyl sulfoxide (8 mL), PEG-NPC (780  $\mu\text{mol}$ ) and TEA (1.17 mmol) were added, and the solution was stirred for 5 days at room temperature under  $\text{N}_2$  atmosphere. The solution was diluted with distilled water and dialyzed using a dialysis bag (molecular weight 12000-14000 cut off) against distilled water for 2 days. The crude compound was lyophilized and then purified by a Sephadex G-75 column [Pharmacia, 4 cm (diameter)  $\times$  45 cm (length)] using 0.1 M  $\text{Na}_2\text{SO}_4$  aqueous



solution as the eluent. The dendrimers were again dialyzed against distilled water for 2 days to remove the salt and lyophilized (351 mg, yield 37.9%). PEG-cys-PAMAM G3 and PEG-cys-PAMAM G4 dendrimers were synthesized using cys-PAMAM G3 and G4 dendrimers according to the same procedure.  $^1\text{H}$  NMR for cystamine core PEG-modified PAMAM dendrimers (400MHz,  $\text{D}_2\text{O}$ ):  $\delta$  2.42 (br, He), 2.63 (br, Hg), 2.82 (br, Hf), 3.26 (m, Hc), 3.30 (m, Hd, Hh), 3.39 (s, Ha), 3.73 (m,  $\text{OCH}_2\text{CH}_2$ ), 4.21 (br, Hb).

#### ***Preparation of GNR-cored PEG-PAMAM dendrimers***

The PEG-modified PAMAM dendrimers with GNR core were prepared according to Scheme 1. An aliquot (25  $\mu\text{L}$ ) of  $\text{HAuCl}_4$  (20 mM) was mixed with 0.1 M CTAB (5 mL) aqueous solution at 27  $^\circ\text{C}$ . An aliquot (16.5  $\mu\text{L}$ ) of  $\text{AgNO}_3$  (6 mM) and 90 mM ascorbic acid (11.1  $\mu\text{L}$ ) solution were added at 27  $^\circ\text{C}$ . Then, 0.5  $\mu\text{L}$   $\text{NaBH}_4$  solution (1 mM in 0.3 M NaOH) was rapidly mixed at 27  $^\circ\text{C}$  and subsequently 0.5 mM PEG-cys-PAMAM dendrimer solution (18.2  $\mu\text{L}$ ) were added into the solution at varying timings after the addition of  $\text{NaBH}_4$ . After 30 min reaction with stirring at 25  $^\circ\text{C}$ , the PEG-modified dendrimers having GNP core were washed twice with centrifugation at 10000 rpm for 10 min, and redispersed in 30 mL distilled water. For further stabilization, PEG-modified PAMAM dendrons with a sulfhydryl group were additionally reacted with the GNP-cored dendrimers. The sulfhydryl-core PEG-modified PAMAM dendrons were prepared by reducing PEG-cys-PAMAM dendrimers (0.5 mM, 72.8  $\mu\text{L}$ ) with 72.8  $\mu\text{L}$   $\text{NaBH}_4$  solution (1 mM in 0.3 M NaOH) for 30 min at room temperature and excess  $\text{NaBH}_4$  was decomposed by adding HCl

(0.3 M, 72.8  $\mu$ L). Then, GNP-cored PEG-modified dendrimers were mixed with the PEG-PAMAM-SH dendron solution and incubated for 48 h at 30  $^{\circ}$ C. The obtained GNR-core PEG-PAMAM dendrimers were purified twice by centrifugation at 8000 rpm for 10 min, and redissolved in distilled water.

#### ***Photothermal effect under NIR laser irradiation***

The aqueous solutions (3 mL) of GNR-cored PEG-modified PAMAM dendrimers ( $[\text{Au}] = 30 \mu\text{M}$ ) were irradiated with a NIR laser (AMAKI,  $\lambda = 808 \text{ nm}$ , 6  $\text{W}/\text{cm}^2$ ). The temperature of sample solution was monitored with a thermometer (SK-1250MC, SATO KEIRYOKI MFG. Co.). The initial temperature of the solution before the laser irradiation was 24  $^{\circ}$ C.

#### ***In vitro cytotoxicity assay***

HeLa cells were seeded into a 24-well microplate ( $5 \times 10^4$  cells/well) with 500  $\mu$ L of Dulbecco's modified Eagle's medium (DMEM) supplemented with 10% FBS 24 h before experiments. Then, an aliquot (500  $\mu$ L) of GNR-core PEG-PAMAM dendrimers or unmodified GNR ( $[\text{Au}] = 0.05\text{-}0.3 \text{ mM}$ ) were added to the cells and incubated for 3 h. Then, the cells were washed with phosphate-buffered saline (PBS) twice, and incubated for another 20 h in 500  $\mu$ L of DMEM supplemented with 10% FBS. The cell viability was determined by using an assay with 3-(4,5-Dimethyl-2-thiazolyl)-2,5-diphenyl-2H-tetrazolium bromide (MTT).<sup>14</sup>

#### ***Evaluation of photo-induced cytotoxicity***

HeLa cells ( $2 \times 10^5$  cells) were seeded into a 35 mm dish in 2 mL of DMEM supplemented with 10% FBS, and cultured for 24 h. The cells were washed with PBS,

and incubated in 2 mL DMEM containing GNR-core PEG-PAMAM G3 dendrimers ([Au] = 0.25 mM) for 3 h. Then, the cells were washed with PBS, immersed in Opti-MEM and then exposed to NIR laser (808 nm, 6 W/cm<sup>2</sup>) for 10 min. Cells were stained with both calcein AM (1.0 µg/mL) and propidium iodide (1.0 µg/mL), which are respectively for alive cells and for damaged cells, in 2 mL DMEM for 30 min. Fluorescence images of HeLa cells were taken using an IMT-2 microscope equipped with an IMT2-RFL fluorescence unit (Olympus). For cell morphology observation using confocal laser scanning microscopy (CLSM) before and after laser irradiation treatment, the HeLa cells with or without 10 min NIR laser irradiation (808 nm, 6 W/cm<sup>2</sup>) were stained with DiI (2.5 µg/mL) in 2 mL DMEM for 15 min. CLSM analysis of the cells was performed on a LSM 5 EXCITER (Carl Zeiss Co. Ltd.).

#### *Anti-tumor effect*

Anti-tumor effect of GNR-core PEG-PAMAM dendrimers was examined as previously reported.<sup>31</sup> Tumor-bearing mice were prepared by inoculating mouse colon carcinoma 26 cells (1x10<sup>6</sup> cells) into both the left and right flanks of BALB/c mice (female, 7 weeks old) under anesthesia and the tumor was allowed to grow for about 10 days, when the volume was approximately 50-200 mm<sup>3</sup>. The dendrimer was injected into the tumors under anesthesia. At 1 h after the injection, the left tumor was locally irradiated with NIR laser (808 nm, 0.24 W/cm<sup>2</sup>) for 10 min. Tumor volumes were determined as

$$\text{Volume} = L \times W^2 / 2$$

where L is the longest dimension parallel to the skin surface and W is the dimension

perpendicular to L and parallel to the surface.

### ***Other measurements***

<sup>1</sup>H NMR spectra were recorded with a JEOL JNM-LA 400. Absorption spectra ranging from 400 nm to 1000 nm were taken with a Jasco Model V-560 spectrophotometer (Jasco Inc., Japan). Transmission electron microscopy (TEM) analysis was performed using JEM-2000FEX II (JEOL Ltd.). Dynamic light scattering (DLS) analysis was performed on a DLS-6000 dynamic light scattering instrument (Otsuka Electronics Co. Ltd.) equipped with an Ar laser ( $\lambda = 488$  nm). GNR-core PEG-PAMAM dendrimers aqueous solution ( $[Au] = 80 \mu\text{M}$ , 2 mL) was used for each measurement. The scattered light intensity was detected at an angle of  $90^\circ$  and analyzed using Marquadt mode. The data present the size distribution of weight frequency. Atomic force microscopy (AFM) measurements (dynamic force mode) were performed by SPI3800 probe station and SPA400 unit system (Seiko Instruments Inc.). The cantilever was made of silicon (SI-DF40; Seiko Instruments Inc.), and its spring constant was 16 N/m.

### **Results and discussion**

We selected PAMAM dendrimers modified with PEG as the dendrimer moiety of GNR-cored dendrimers, considering their potential application to biomedicine. The attachment of PEG chains is well known to improve the biocompatibility of material surfaces. In addition, PEG-modification can increase the colloidal stability of nanoparticles in storage and in the physiological fluids. An earlier study demonstrated

that amine-terminated PAMAM dendrimers can be fully modified with PEG by reaction with PEG-NPC.<sup>10</sup> We applied the same method in this study to amine-terminated PAMAM dendrimers with cystamine core, which revealed that PEG-modification was achieved for the cystamine-core PAMAM dendrimers as reported previously using NMR.<sup>10</sup>

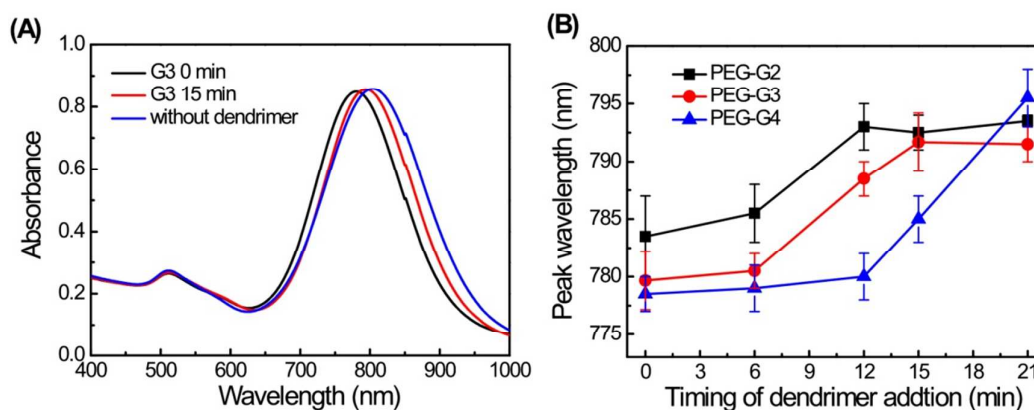


Figure 1. (A) Absorption spectra of GNRs synthesized without and with addition of PEG-cys-PAMAM G3 dendrimers at 0 min and 15 min after the initiation of the reaction. (B) Longitudinal plasmon peak wavelength of GNRs synthesized with addition of PEG-cys-PAMAM G2, G3, and G4 dendrimers as a function of the dendrimer addition timing. All spectra were measured after the 30 min-reaction.

Previous reports have described that GNP-cored dendrimers can be prepared by GNP production with  $\text{NaBH}_4$  in the presence of dendrimers with disulfide core.<sup>32</sup> The S–S bond of the disulfide will be broken during adsorption onto the gold surface resulting in individual dendrons stabilizing the metallic nanoparticle.<sup>33</sup> Therefore, in this study, we prepared GNRs in the presence of cys-PAMAM dendrimers of various generations (Scheme 1). Although GNRs have been prepared using various methods, the seed-mediated growth method is the most widely used. In that method, GNRs are formed by anisotropic growth of a gold seed coated by a CTAB bilayer.<sup>34</sup> Therefore,

we expected that the attachment of the PEG-modified PAMAM dendrons onto the growing GNR might suppress further growth of the GNRs, resulting in their conjugates with small GNR. The GNR preparation was conducted by adding  $\text{NaBH}_4$  into a mixture aqueous solution composed of CTAB,  $\text{HAuCl}_4$ ,  $\text{AgNO}_3$ , and ascorbic acid.<sup>35</sup> In this process, GNRs grow with time. Their growth was completed in 30 min. Therefore, we added PEG-cys-PAMAM dendrimers to the reaction mixture at various timings between 0 and 21 min after initiation of the GNR growing process (Scheme 1).

The effects of addition of the dendrimers to GNRs were investigated from their absorption spectra. Fig. 1A shows typical absorption spectra of GNRs prepared without or with the addition of PEG-cys-PAMAM G3 dendrimer at 0 min and 15 min after initiation of the reaction. Compared with the GNRs synthesized without dendrimers, the addition of PEG-cys-PAMAM G3 dendrimers at the timing of 0 min and 15 min caused the blue-shift of peak wavelength. The result indicates that addition of the PEG-cys-PAMAM dendrimers affects the SPR properties of the resultant GNRs. The relation between the longitudinal plasmon peak wavelength and the timing of the dendrimer addition was examined further using PEG-cys-PAMAM dendrimers of different generations (Fig. 1B). Irrespective of the dendrimer generation, addition of the dendrimers to the GNR formation reaction mixture without the delay time induced marked shortening of SPR of the longitudinal mode for the resultant GNRs. The SPR peak wavelength increased gradually with increasing delay time before the addition of the dendrimers into the reaction mixture, which suggests

that these PEG-cys-PAMAM dendrimers reacted with GNRs during their growth. That reaction affected their SPR properties. The SPR of GNRs in the longitudinal mode is known to be affected by their ratio of length to width: their aspect ratio.<sup>36</sup> Therefore, the observed shortening of the SPR wavelength for the GNPs with the dendrimers might indicate that the reaction with the dendrimers induced generation of GNRs with a decreased aspect ratio. Considering that the disulfide core of the dendrimers is easily reduced by ascorbic acid, the reduction of PEG-cys-PAMAM dendrimers is likely to generate their derived dendrons with a thiol group at focal point, which reacted with the immature GNRs during their growth and which suppressed their further growth.

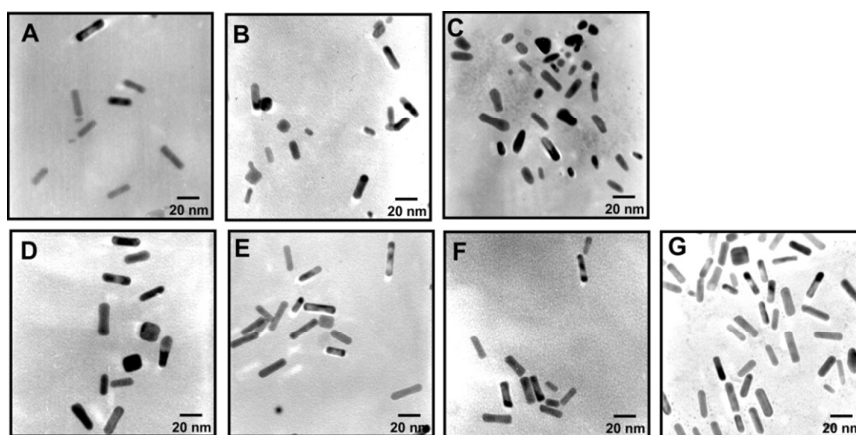


Figure 2. Typical TEM images GNRs prepared with PEG-cys-PAMAM G2 (A,D), G3 (B,E) and G4 (C,F) dendrimers without the delay time (A,B,C) or with the delay time of 15 min (D,E,F) and GNRs prepared without dendrimer (G). Scale bars are 20 nm.

Transmission electron microscopy (TEM) was used to investigate the sizes of the GNRs prepared with or without dendrimers (Fig. 2). The GNRs prepared without dendrimer showed a rod-like shape with about 25 nm length and 6.5 nm width (Fig.

2G). In contrast, GNRs prepared with dendrimers without the delay time were smaller rod-like particles (Figs. 2A–2C), indicating that attachment of the dendrimers to the immature GNRs might strongly suppress their further growth. However, the GNRs prepared with dendrimers with delay time of 15 min exhibited almost identical size and morphology to those prepared without dendrimers (Figs. 2D–2F). Probably, GNR formation proceeded to their mature form in 15 min before the addition of the dendrimers. Therefore, attachment of the dendrons to the almost-matured GNRs did not affect their morphology.

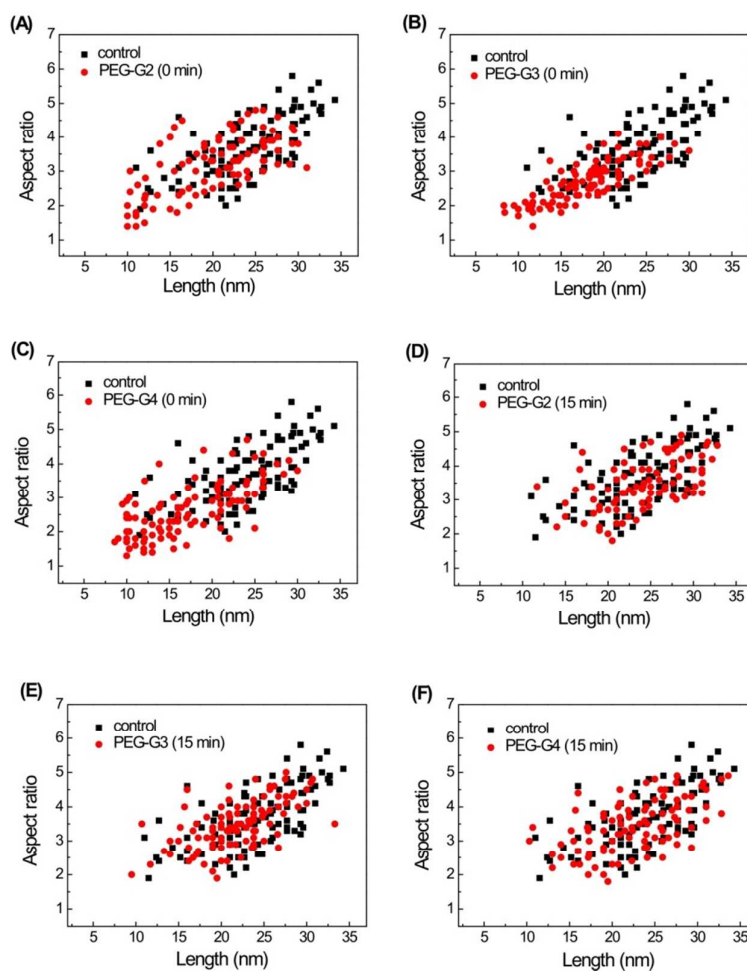


Figure 3. Relationship between length and aspect ratio for GNRs prepared with and PEG-cys-PAMAM G2 (A,D) G3 (B,E) and G4 (C,F) dendrimers without the delay time (A,B,C) or with the delay time of 15 min (D,E,F). Data for GNRs prepared



without dendrimers are also given in each figure as a control.

Based on the TEM images, we estimated the size and aspect ratio for the GNRs. Their relation is depicted in Fig. 3. The GNRs prepared without GNRs exhibited large particle sizes of 20–30 nm. In contrast, the GNRs prepared with the dendrimers without the delay time showed mostly shorter particles of 10–25 nm, again indicating a reduction of particle size via attachment of the dendrons (Figs. 3A–3C). However, when prepared with the dendrimers with the delay time of 15 min, the GNRs exhibited an almost identical size and aspect ratio distribution to those prepared without dendrimers (Figs. 3D–3F). Irrespective of the presence or absence of dendrimers during the GNR production, all the GNRs seem to exhibit a linear relation between the length and aspect ratio (Figs. 3A–3F). This fact suggests that the aspect ratio of the GNRs increases linearly with increasing length and that the attachment of the dendrons did not disturb this relation. Considering that GNRs are growing from specific crystallographic facets of the seeds and /or rods, it is likely that dendrons with a Au-reactive thiol group might react to these facets and prohibit further growth of the GNRs, resulting in shorter GNRs with a lower aspect ratio. Based on the TEM analysis, the average length and aspect ratio for these GNRs are presented in Table 1. It is apparent that PEG-dendron-attached GNRs with size similar to that of PEG-modified dendrons (around 18 nm) is obtainable by GNR formation in the presence of the dendrimers. Considering their application to biomedical fields, dendrimer-like particles consisting of PEG-modified dendrons and small GNR core can be of great interest from the viewpoint of colloidal stability and controllability of

the biodistribution. Therefore, we used these PEG-dendrimer-attached GNRs for additional experiments.

Table 1. Average length and aspect ratio for GNRs prepared with or w/o dendrimers added 0 min or 15 min after starting GNR growth

dendrimer	0 min (nm)	Aspect ratio	15 min (nm)	Aspect ratio
G2	20.0±6.4	3.2	27.4±4.7	3.6
G3	18.5±4.4	2.9	25.0±5.7	3.7
G4	18.2±5.8	2.8	24.2±5.8	3.5
w/o dendrimer	24.0±3.5	3.7		

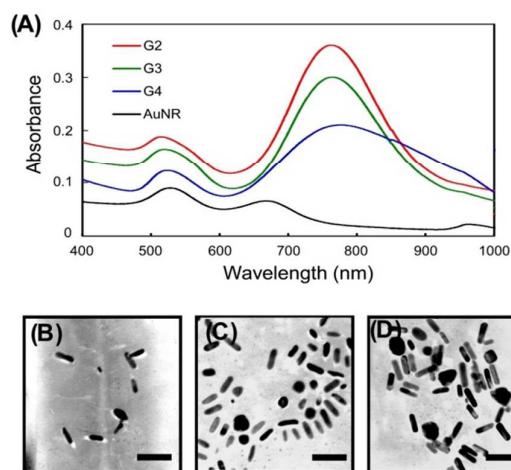


Figure 4. (A) Typical absorption spectra of PEG-PAMAM G2 dendron-attached GNRs, PEG-PAMAM G3 dendron-attached GNRs, PEG-PAMAM G4 dendron-attached GNRs, and GNRs without dendrons. TEM images of (B) PEG-PAMAM G2 dendron-attached GNRs, (C) PEG-PAMAM G3 dendron-attached GNRs, and (D) PEG-PAMAM G4 dendron-attached GNRs. Both absorption spectra and TEM images of GNRs were measured after 48 h incubation without or with dendrons, followed by two cycles of centrifugation. The scale bar in TEM images is 30 nm.

We observed that the peak wavelength of the dendron-attached GNRs became shorter, about 650 nm, during incubation at 25°C for 2 days, probably because of their aggregation. Therefore, we additionally reacted PEG-PAMAM dendrons with a thiol

group at focal point to the dendron attached GNRs to improve their colloidal stability (see the Experimental section). These dendron-attached GNRs were washed with distilled water using centrifugation. Then their absorption spectra were measured (Fig. 4A). Whereas the unmodified GNRs prepared without dendrimer showed the longitudinal SPR with peak wavelength at 807 nm immediately after the synthesis (Fig. 1A), the peak wavelength moved to 681 nm after 48 h incubation (Fig. 4A). This 133 nm blue shift of longitudinal SPR peak was previously reported as attributable to the reshaping of the GNRs in an aqueous environment.<sup>37</sup> In contrast, the Au NRs stabilized by PEG-PAMAM G2 and PEG-PAMAM G3 dendrons showed only a slight blue shift of longitudinal SPR peak, suggesting that the GNR moiety is covered efficiently with the PEG-dendrons and provided with high colloidal stability. However, the PEG-G4-PAMAM dendron-attached GNR showed a broad longitudinal SPR absorption, indicating that the aggregation of GNRs was induced during the centrifugation. Compared with PEG-PAMAM G2 and G3 dendrons, larger size and higher PEG density of PEG-PAMAM G4 dendron might show stronger steric repulsion, resulting in the inefficient conjugation to the GNRs and insufficient stabilization of GNRs. Colloidal stability of these PEG-PAMAM dendron-attached GNRs was further confirmed by TEM images. The PEG-PAMAM G2-attached GNRs (Fig. 4B) and PEG-PAMAM G3-attached GNRs (Fig. 4C) displayed individually dispersed GNRs, although aggregation of GNRs was observed for PEG-PAMAM G4-attached GNRs (Fig. 4D).

Morphology of the PEG-PAMAM dendron-attached GNR was also investigated

using atomic force microscopy (AFM) to confirm the presence of conjugated PEG-PAMAM dendrons layer (Fig. 5). AFM images for PEG-PAMAM G2 dendron-attached GNR showed discrete entities of about 20 nm (Figs. 5A and 5D). Instead of the clear cylindrical shapes of GNR core moiety observed in TEM images (Fig. 4), ellipsoidal particles for PEG-PAMAM-G2 dendron-attached GNRs were observed (Fig. 5D). Similarly, well-dispersed particles with about 30 nm were observed in AFM images of PEG-PAMAM G3 dendron-attached GNR, although these particles were spherical (Figs. 5B and 5E). These shape changes were probably caused by the attachment of the highly hydrated dendron layer on the GNRs, which might result in decrease of the aspect ratio compared to their GNR core alone. It is noteworthy that the PEG-PAMAM G3 dendron-attached GNRs showed spherical morphologies in contrast to the ellipsoidal morphologies of the PEG-PAMAM G2 dendron-attached GNRs, which might indicate that the PEG-PAMAM G3 dendron formed higher density layer of PEG chains on the GNR surface than PEG-PAMAM G2 dendron. In contrast, AFM images for GNR-core PEG-PAMAM G4 dendrimers clearly showed aggregates of several particles (Figs. 5C and 5F), which is consistent with the TEM observation (Fig. 4D).

The PEG-PAMAM dendron-attached GNR size was further investigated using dynamic light scattering (DLS). The PEG-PAMAM G2 dendron-attached GNR, PEG-PAMAM G3 dendron-attached GNR, and PEG-PAMAM G4 dendron-attached GNR were estimated respectively as having diameters of  $24.3 \pm 9$  nm,  $31.2 \pm 13.4$  nm, and  $77.7 \pm 29.7$  nm (Figs. 5G–5I). These particle sizes agree with the AFM

observations (Figs. 5D–5F). Nanoparticles with ellipsoidal shapes might be approximated as a translationally diffusing sphere whose diameter equaled the length of nanorod, because their rotational diffusion is rapid.<sup>38</sup> We also measured sizes of PEG-modified PAMAM G2, G3, and G4 dendrimers using DLS and found that their z-average diameters were, respectively, 13.2, 15.4, and 17.6 nm. Assuming that the PEG-dendrons attached to the GNR and those forming the dendrimers have equal size, the structures of the PEG-PAMAM G3 dendron-attached GNR with a spherical shape can be regarded as GNR-core PEG-PAMAM dendrimers (Fig. 5J).

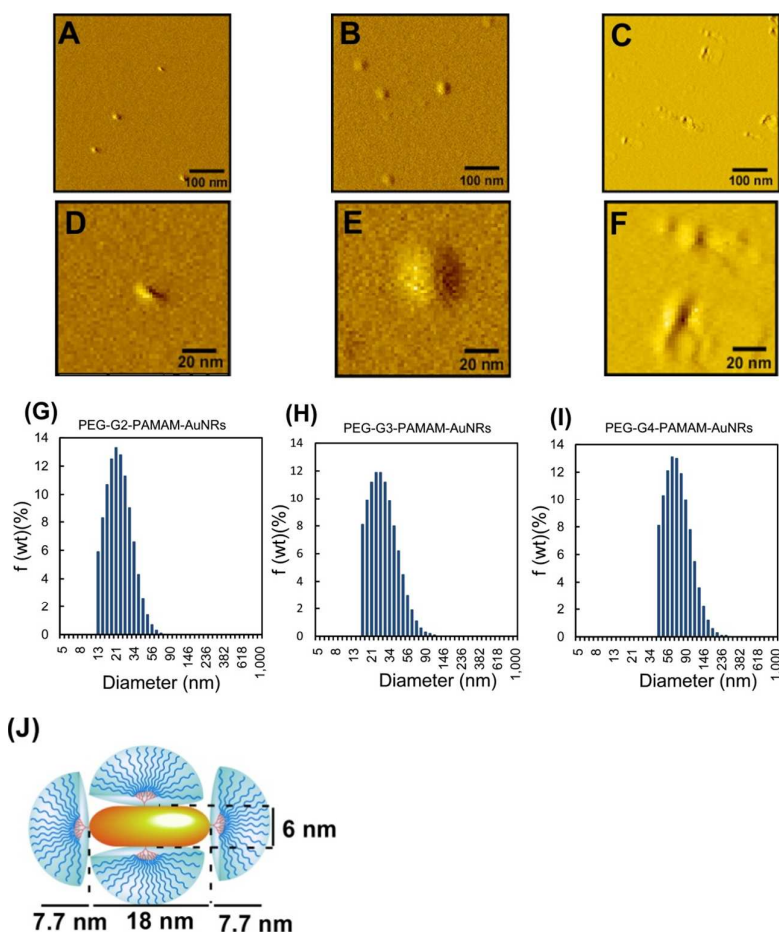


Figure 5. AFM images of PEG-PAMAM G2 (A, D), G3 (B, E), and G4 (C, F) dendron-attached GNRs. Size distributions of PEG-PAMAM G2 (G), G3 (H), and G4 (I) dendron-attached GNRs based on DLS measurements. (J) Schematic illustration of structure of PEG-PAMAM G3 dendron-attached GNR.

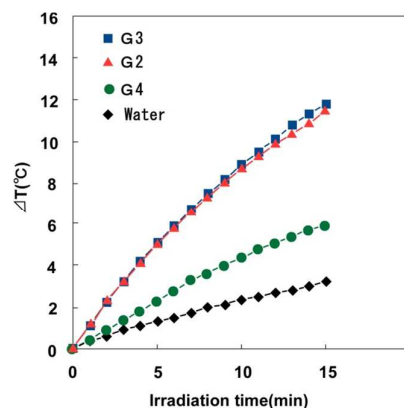


Figure 6. Temperature increment of water and aqueous PEG-PAMAM G2, G3 and G4 dendron-attached GNR solutions under 808 nm laser irradiation ( $6 \text{ W/cm}^2$ ). Initial temperature was  $24^\circ \text{C}$ . Au concentration was  $30 \mu\text{M}$ .

Considering the application of the GNR-core PEG-PAMAM dendrimer to biomedicine, their photothermal properties are important. Therefore, we compared its heat generating ability to that of GNR modified with PEG-PAMAM G2 to G4 dendrons under irradiation of NIR light. As presented in Fig. 6, an aqueous solution of GNR-core PEG-PAMAM G3 dendrimer showed a temperature increase by about  $13^\circ \text{C}$  during 15 min application of NIR irradiation ( $\lambda = 808 \text{ nm}$ ,  $6 \text{ W/cm}^2$ ). A similar temperature increase was observed for the PEG-PAMAM G2 dendron attached GNR solution, but the PEG-PAMAM G4 dendron attached GNR exhibited much lower extent of temperature increase. Considering that only GNR modified with PEG-PAMAM G4 dendron formed aggregates among GNRs having PEG-PAMAM dendrons of various generations (Fig. 5), the high colloidal stability of GNRs with PEG-PAMAM dendron might be crucial for the excellent heat generating capability of the GNR core.

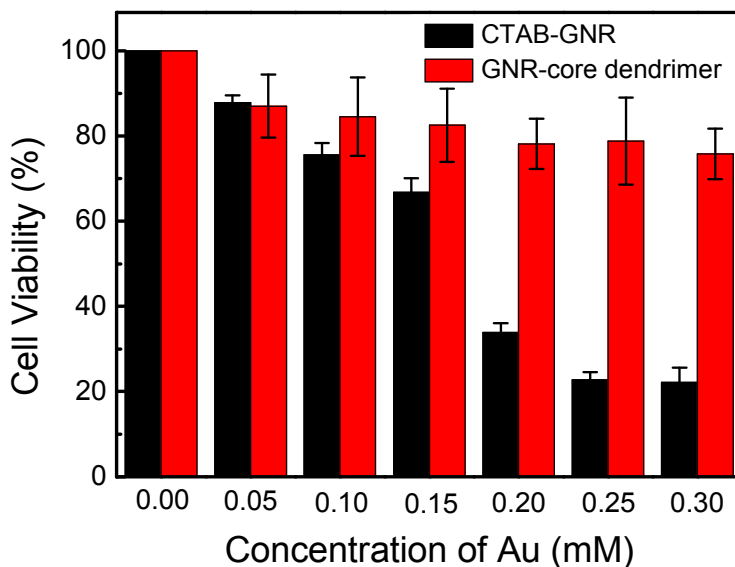


Figure 7. Cytotoxicity of unmodified GNR and GNR-core PEG-PAMAM G3 dendrimer to HeLa cells at different Au concentrations. Data are given as the mean  $\pm$  SD (n=3).

The *in vitro* cytotoxicity of the GNR-cored PEG-PAMAM G3 dendrimer was examined using human cervical cancer-derived HeLa cells using the MTT assay and was compared with that of GNR prepared without PEG-sys-dendrimer, which were used as a control (Fig. 7). The unmodified GNR increased its cytotoxicity with increasing concentration and showed quite high cytotoxicity at Au concentrations above 0.25 mM, where only 20% of cells survived. In contrast, more than 80% of the cells survived for those treated with the GNR-cored PEG-PAMAM G3 dendrimer under the same experimental conditions, indicating the low cytotoxicity of the GNR-cored PAMAM G3 dendrimer.

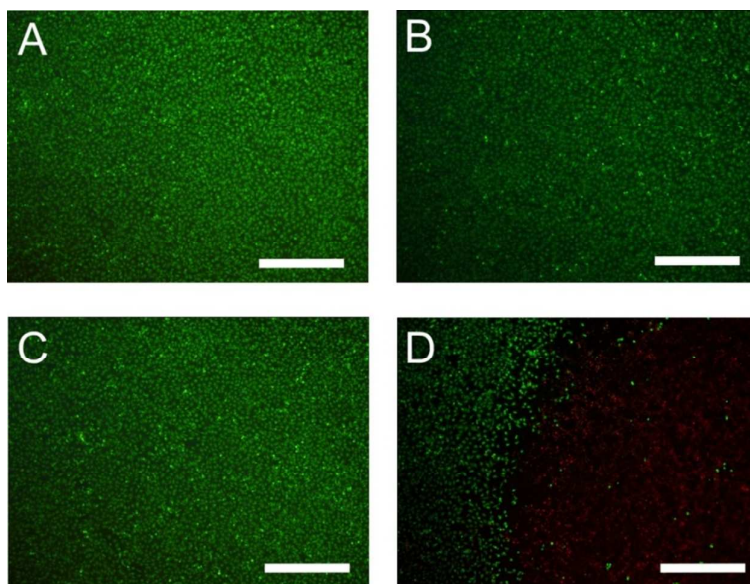


Figure 8. Fluorescence microscopic observation of NIR-induced cell-killing by GNR-core PEG-PAMAM G3 dendrimer. HeLa cells were treated with GNR-core PEG-PAMAM G3 dendrimer for 3 h at Au concentration of 0.25 mM, washed with PBS and irradiated with NIR laser ( $\lambda=808$  nm,  $6$  W/cm<sup>2</sup>) for 10 min. Cells without (A,C) and with (B,D) dendrimer treatment before (A,B) and after (C,D) NIR laser irradiation were stained with calcein-AM and propidium iodide and observed using a fluorescence microscope. The scale bar represents 1 mm. Calcein-AM fluorescence (green) and propidium iodide fluorescence (red) respectively show living and dead cells.

Photoactivated cell-killing capability of the GNR-core PEG-PAMAM G3 dendrimer was examined by comparing the effects of NIR laser irradiation on cellular survival among HeLa cells with and without dendrimer treatment (Fig. 8). The HeLa cells showed damage neither with the dendrimer treatment alone (Fig. 8B) nor with NIR laser irradiation alone (Fig. 8C). However, the cells treated with the dendrimer and irradiated with NIR laser exhibited considerable damage. However, the cells treated with the GNR-core PEG-PAMAM G3 dendrimer and irradiated with NIR laser exhibited considerable damage (Fig. 8D). The cells around the laser light irradiated area displayed red fluorescence, indicating that almost all cells had been killed by laser irradiation. Indeed, the GNR-core PEG-PAMAM G3 dendrimer exhibited strong



heat-generating ability under NIR irradiation (Fig. 6). The observed cell death might be induced through the heat generated from GNR core of the dendrimer activated with NIR irradiation.

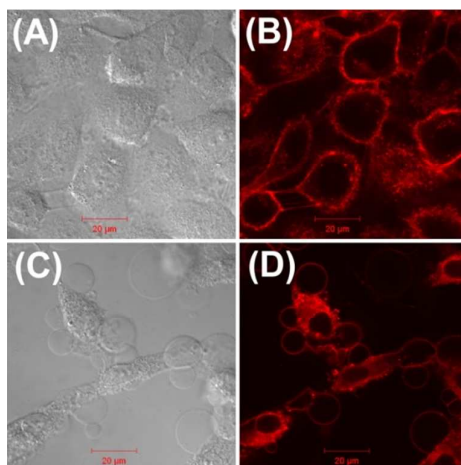


Figure 9. CLSM images of HeLa cells stained with DiI. HeLa cells were treated with GNR-core PEG-PAMAM G3 dendrimer for 3 h at Au concentration of 0.25 mM, washed with PBS, and observed immediately (A,B) or after NIR laser ( $\lambda=808$  nm, 6 W/cm<sup>2</sup>) irradiation for 10 min (C,D) using CLSM.

It has been reported that laser irradiation of nanorods internalized in a cell can lead to cell apoptosis by inducing mitochondria damage or plasma membrane integrity.<sup>39</sup> Therefore, morphology of the cells treated with GNR-core PEG-PAMAM G3 dendrimers with and without laser irradiation was further observed using CLSM. A lipophilic dye DiI was used to stain cell membranes. As shown in Fig. 9, blebs appeared on surface of the cells irradiated with laser, although no blebs were observed for those without laser irradiation (Fig. 9). These blebs might be generated from the cell membranes due to the cavitation effects induced by GNRs-mediated rapid rise in temperature and superheating for the cells under laser irradiation.<sup>40</sup> As a result, necrosis of the cell might be induced by GNR-core PEG-PAMAM

dendrimers-mediated photothermolysis, which was accomplished with the blebbing and disruption of the cellular membrane.

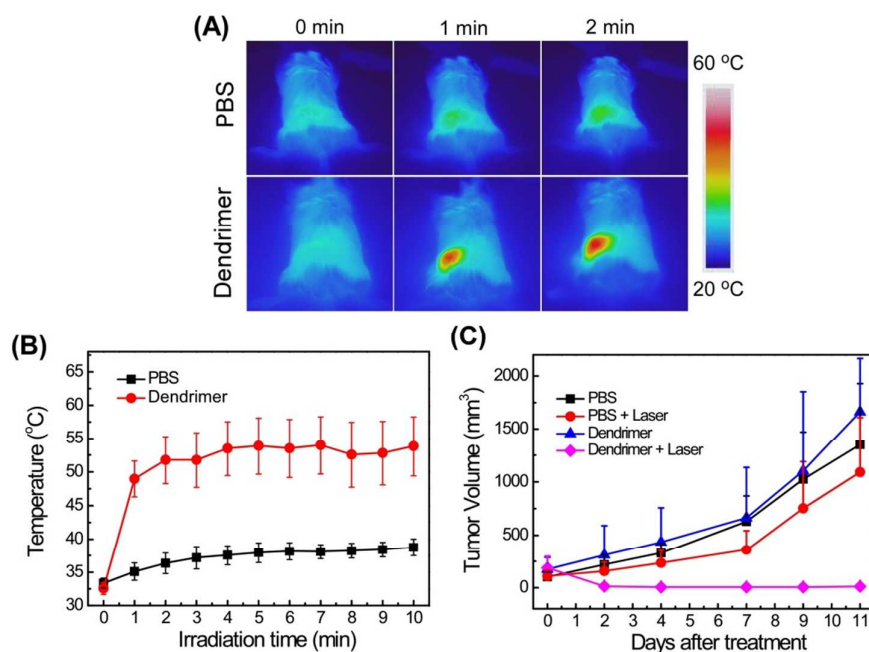


Figure 10. Photothermal effects of GNR-core PEG-PAMAM G3 dendrimer on tumor suppression for mice having colon carcinoma 26 tumors. Tumors were injected with GNR-core PEG-PAMAM G3 dendrimer or PBS and the left tumors were irradiated with NIR laser ( $\lambda=808$  nm,  $0.24$  W/cm<sup>2</sup>) for 10 min. (A) Thermographic images of tumors before and 1 min and 2 min after NIR laser irradiation. (B) Time courses of temperature of the left tumor injected with the dendrimer or PBS under NIR laser irradiation. (C) Time courses for volumes of tumors with various treatments. Six mice per group were used and data were given as mean  $\pm$  SD ( $n=6$ ) (B, C).

Based on the excellent photothermal effects of the GNR-core PEG-PAMAM G3 dendrimer to tumor cells *in vitro*, we examined its anti-tumor performance further *in vivo*. We prepared mice bearing tumors by inoculating mouse colon carcinoma 26 cells into both the left and right flanks of BALB/c mice. The GNR-core PEG-PAMAM G3 dendrimer or PBS was injected into the tumors, and the left tumors were irradiated with an NIR laser for 10 min. The right tumors without laser

irradiation were used as control. During irradiation, thermographs were recorded using an NIR thermal camera. As shown in Figs. 10 A and 10 B, only the tumors treated with GNR-core PEG-PAMAM G3 dendrimer and irradiated with NIR laser exhibited a rapid temperature increase to above 50°C within 2 min. However, the PBS-treated tumors with the same laser irradiation showed an average temperature of 38.7 °C, and no obvious temperature change was observed in all right tumors that were not irradiated with the laser. The *in vivo* therapeutic efficacy of GNR-core PEG-PAMAM G3 dendrimer under laser irradiation was assessed by examination of the tumor growth. Fig. 10 C shows that GNR-core PEG-PAMAM G3 dendrimer with laser irradiation group exhibited significant tumor ablation and tumor growth suppression effects: no apparent left tumor was observed for any of 6 mice on day 11 in this group. In contrast, the mice injected with GNR-core PEG-PAMAM G3 dendrimer without laser irradiation showed no marked changes of the tumor growth rate compared with their control mice (injected with PBS without irradiation), indicating the low toxicity of GNR-core PEG-PAMAM G3 dendrimer for the *in vivo* application. Although a slight tumor growth delay was observed for mice tumors treated with PBS with laser irradiation compared to those treated with PBS without irradiation, the tumor ablation effect was not observed. Considering that the dendrimer-injected tumor tissues were maintained above 50°C during the NIR laser irradiation, the strong tumor ablation and tumor growth suppression might be derived from the excellent photothermal capability of the GNR-core dendrimer.

## Conclusions

For this study, we developed a new type of hybrid dendrimer consisting of GNR core around 18–25 nm and PEG-modified PAMAM (PEG-PAMAM) dendrons by the reaction of PEG-PAMAM dendrimers with cystamine core with GNR in the growing process. The hybrid size was shown to be controllable in the nanometer range by selecting the generation of the dendrimers and addition timing of the dendrimer to the growing GNR. Especially, the use of PEG-PAMAM G3 dendrimer produced a spherical hybrid dendrimer with approximately 31 nm diameter in which a small GNR core was well stabilized by the highly hydrated PEG-PAMAM G3 dendrons. The GNR-core PEG-PAMAM dendrimer showed little cell cytotoxicity and strong selective cell-killing capability under NIR laser irradiation. Indeed, this hybrid dendrimer generated heat and caused the remarkable temperature increase of the tumor tissue of the tumor, which was irradiated with a NIR laser, resulting in considerable tumor volume reduction. Considering that PEG-PAMAM dendrimers have high performance as drug carriers, the GNR-core PEG-PAMAM dendrimers containing photothermal components might be useful as a tool for the combination of photothermal therapy and chemotherapy. Indeed, several studies have developed hybrid-type dendrimers with gold nanoparticles. However, these hybrid dendrimers can exhibit photothermal properties only responding to the visible light, which cannot penetrate into body. Considering the advantage of NIR light-responsive property, these GNR-core PEG-PAMAM dendrimers might be attractive as a new nanomaterial for advanced biomedical applications.

## Acknowledgments

This work was supported in part by a Grant-in-aid for Scientific Research from the Ministry of Education, Science, Sports, and Culture in Japan and by a Japan Science and Technology Agency.

## References: References:

- 1 D. A. Tomalia, H. Baker, J. Dewald, M. Hall, G. Kallos, S. Martin, J. Roeck, J. Ryder and P. Smith, *Polym. J.*, 1985, **17**, 117-132.
- 2 D. A. Tomalia, A. M. Naylor and W. A. Goddard, *Angew. Chem., Int. Ed.*, 1990, **29**, 138-175.
- 3 M. Liu and J. M. J. Fréchet, *Pharm. Sci. Technol. Today*, 1999, **2**, 393-401.
- 4 S. M. Grayson and J. M. J. Fréchet, *Chem. Rev.*, 2001, **101**, 3819-3868.
- 5 S.-E. Stiriba, H. Frey and R. Haag, *Angew. Chem., Int. Ed.*, 2002, **41**, 1329-1334.
- 6 U. Boas and P. M. H. Heegaard, *Chem. Soc. Rev.*, 2004, **33**, 43-63.
- 7 S. H. Medina and M. E. H. El-Sayed, *Chem. Rev.*, 2009, **109**, 3141-3157.
- 8 Y. Cheng, L. Zhao, Y. Li and T. Xu, *Chem. Soc. Rev.*, 2011, **40**, 2673-2703.
- 9 K. Kono, *Polym. J.*, 2012, **44**, 531-540.
- 10 C. Kojima, K. Kono, K. Maruyama and T. Takagishi, *Bioconjugate Chem.*, 2000, **11**, 910-917.
- 11 D. Astruc, E. Boisselier and C. Ornelas, *Chem. Rev.*, 2010, **110**, 1857-1959.
- 12 Y. Z. You, C. Y. Hong, C. Y. Pan and P. H. Wang, *Adv. Mater.*, 2004, **16**,

1953-1957.

13 Y. Haba, A. Harada, T. Takagishi and K. Kono, *J. Am. Chem. Soc.*, 2004, **126**, 12760-12761.

14 X. Li, Y. Haba, K. Ochi, E. Yuba, A. Harada and K. Kono, *Bioconjugate Chem.*, 2013, **24**, 282-290.

15 D. Grebel-Koehler, D. Liu, S. De Feyter, V. Enkelmann, T. Weil, C. Engels, C. Samyn, K. Müllen and F. C. De Schryver, *Macromolecules*, 2003, **36**, 578-590.

16 D. A. Tomalia, B. Huang, D. R. Swanson, H. M. Brothers Ii and J. W. Klimash, *Tetrahedron*, 2003, **59**, 3799-3813.

17 Y. Haba, C. Kojima, A. Harada, T. Ura, H. Horinaka and K. Kono, *Langmuir*, 2007, **23**, 5243-5246.

18 J. Zheng, C. Zhang and R. M. Dickson, *Phys. Rev. Lett.*, 2004, **93**, 077402.

19 Y. Zhao, Y. Li, Y. Song, W. Jiang, Z. Wu, Y. A. Wang, J. Sun and J. Wang, *J Colloid Interface Sci.*, 2009, **339**, 336-343.

20 C. Kojima, Y. Umeda, M. Ogawa, A. Harada, Y. Magata and K. Kono, *Nanotechnology*, 2010, **21**, 245104.

21 L. M. Bronstein and Z. B. Shifrina, *Chem. Rev.*, 2011, **111**, 5301-5344.

22 S. Nakao, K. Torigoe, K. Kon-No and T. Yonezawa, *J. Phys. Chem. B*, 2002, **106**, 12097-12100.

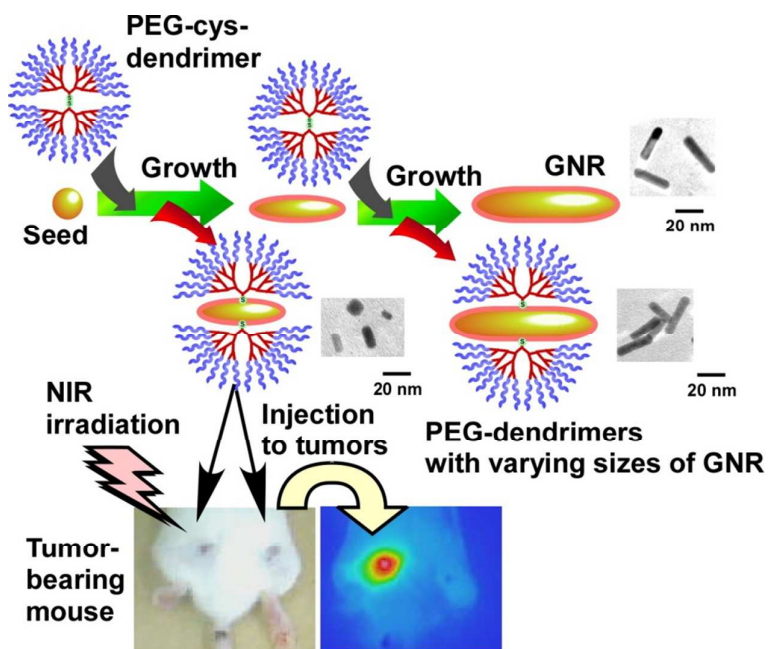
23 Y.-S. Shon, D. Choi, J. Dare and T. Dinh, *Langmuir*, 2008, **24**, 6924-6931.

24 C. S. Love, I. Ashworth, C. Brennan, V. Chechik and D. K. Smith, *J Colloid Interface Sci.*, 2006, **302**, 178-186.

- 25 B. Huang and D. A. Tomalia, *J Lumin.*, 2005, **111**, 215-223.
- 26 A. Harada, A. Yuzawa, T. Kato, C. Kojima and K. Kono, *J. Polym. Sci. Part A: Polym. Chem.*, 2010, **48**, 1391-1398.
- 27 S. Sortino, *J. Mater. Chem.*, 2012, **22**, 301-318.
- 28 R. Weissleder, *Nat. Biotechnol.*, 2001, **19**, 316-317.
- 29 M. Hu, J. Chen, Z.-Y. Li, L. Au, G. V. Hartland, X. Li, M. Marquez and Y. Xia, *Chem. Soc. Rev.*, 2006, **35**, 1084-1094.
- 30 H. Chen, L. Shao, Q. Li and J. Wang, *Chem. Soc. Rev.*, 2013, **42**, 2679-2724.
- 31 K. Kono, T. Ozawa, T. Yoshida, F. Ozaki, Y. Ishizaka, K. Maruyama, C. Kojima, A. Harada and S. Aoshima, *Biomaterials*, 2010, **31**, 7096-7105.
- 32 C. S. Love, V. Chechik, D. K. Smith and C. Brennan, *J. Mater. Chem.*, 2004, **14**, 919-923.
- 33 L. A. Porter, D. Ji, S. L. Westcott, M. Graupe, R. S. Czernuszewicz, N. J. Halas and T. R. Lee, *Langmuir*, 1998, **14**, 7378-7386.
- 34 T. K. Sau and A. L. Rogach, *Adv. Mater.*, 2010, **22**, 1781-1804.
- 35 N. R. Jana, *Small*, 2005, **1**, 875-882.
- 36 Y.-Y. Yu, S.-S. Chang, C.-L. Lee and C. R. C. Wang, *J. Phys. Chem. B*, 1997, **101**, 6661-6664.
- 37 M. Iqbal and G. Tae, *J. Nanosci. Nanotechnol.*, 2006, **6**, 3355-3359.
- 38 S. E. Lee, D. Y. Sasaki, T. D. Perroud, D. Yoo, K. D. Patel and L. P. Lee, *J. Am. Chem. Soc.*, 2009, **131**, 14066-14074.
- 39 L. Tong and J.-X. Cheng, *Nanomedicine*, 2009, **4**, 265-276.

40 L. Tong, Q. Wei, A. Wei and J.-X. Cheng, *Photochem. Photobiol.*, 2009, **85**, 21-32.



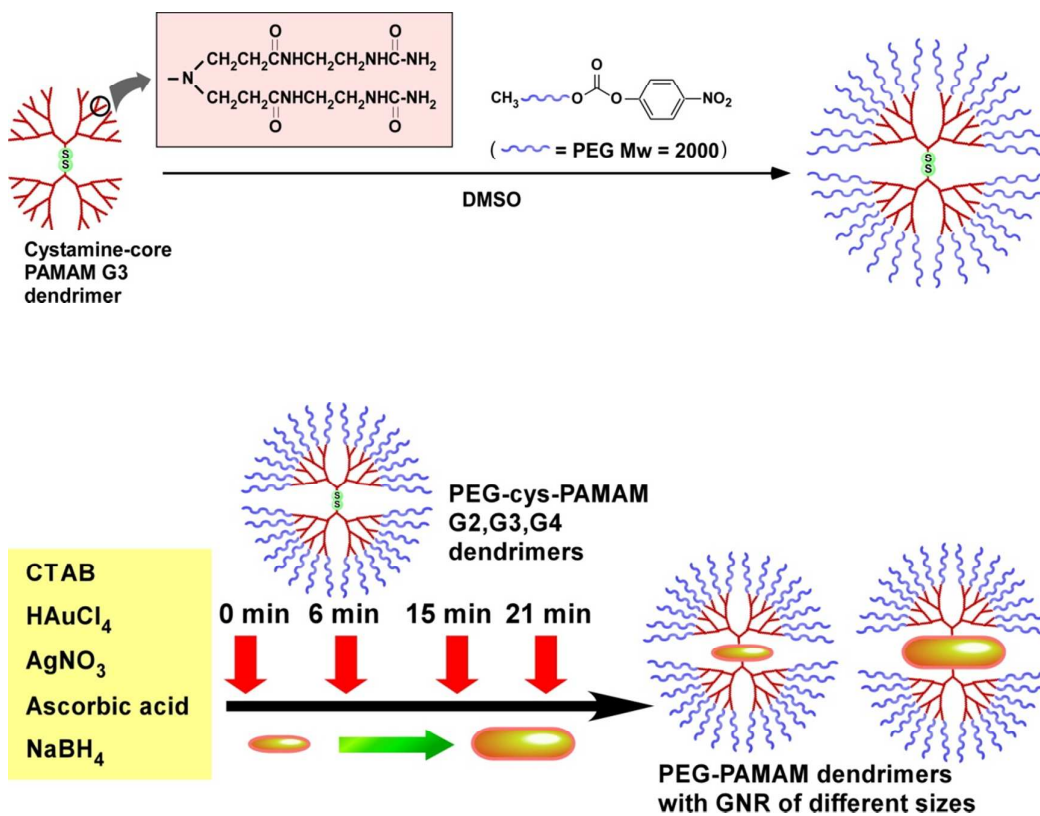


A new type of hybrid dendrimers consisting of a gold nanorod core and polyethylene glycol-modified polyamidoamine dendrons was developed for biomedical applications such as photothermal therapy.

Graphic for abstract

**Table 1. Average length and aspect ratio for GNRs prepared with or w/o dendrimers added 0 min or 15 min after starting GNR growth**

dendrimer	0 min (nm)	Aspect ratio	15 min (nm)	Aspect ratio
G2	20.0±6.4	3.2	27.4±4.7	3.6
G3	18.5±4.4	2.9	25.0±5.7	3.7
G4	18.2±5.8	2.8	24.2±5.8	3.5
w/o dendrimer	24.0±3.5	3.7		



Scheme 1. Synthesis of PEG-cys-PAMAM dendrimers and GNR-core PEG-PAMAM dendrimers.

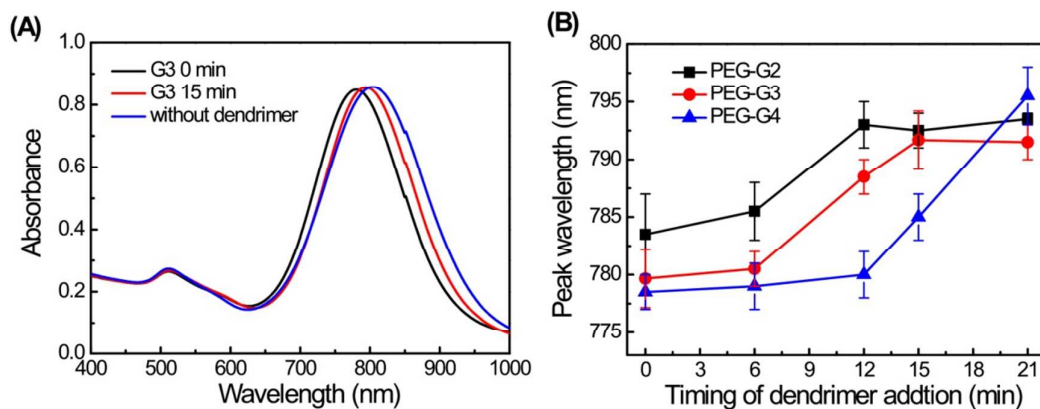


Figure 1. (A) Absorption spectra of GNRs synthesized without and with addition of PEG-cys-PAMAM G3 dendrimers at 0 min and 15 min after the initiation of the reaction. (B) Longitudinal plasmon peak wavelength of GNRs synthesized with addition of PEG-cys-PAMAM G2, G3, and G4 dendrimers as a function of the dendrimer addition timing. All spectra were measured after the 30 min-reaction.

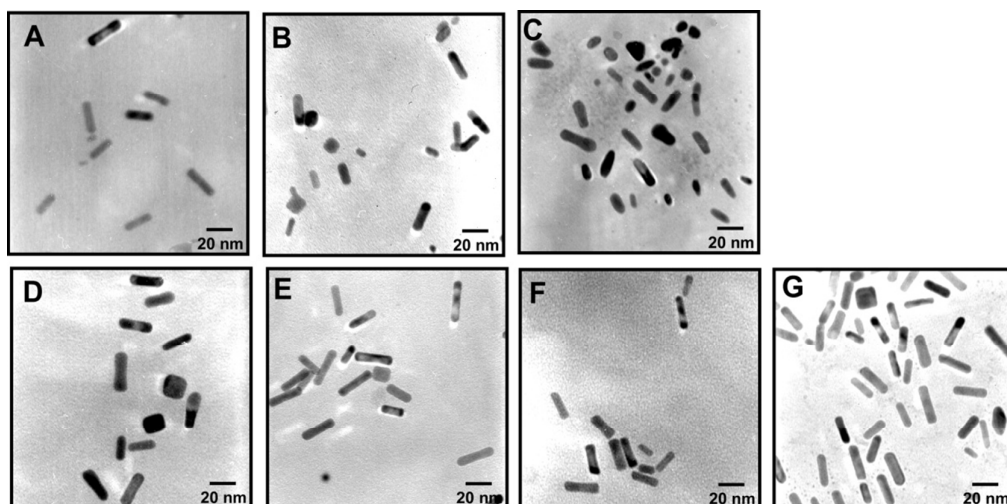


Figure 2. Typical TEM images GNRs prepared with PEG-cys-PAMAM G2 (A,D), G3 (B,E) and G4 (C,F) dendrimers without the delay time (A,B,C) or with the delay time of 15 min (D,E,F) and GNRs prepared without dendrimer (G). Scale bars are 20 nm.

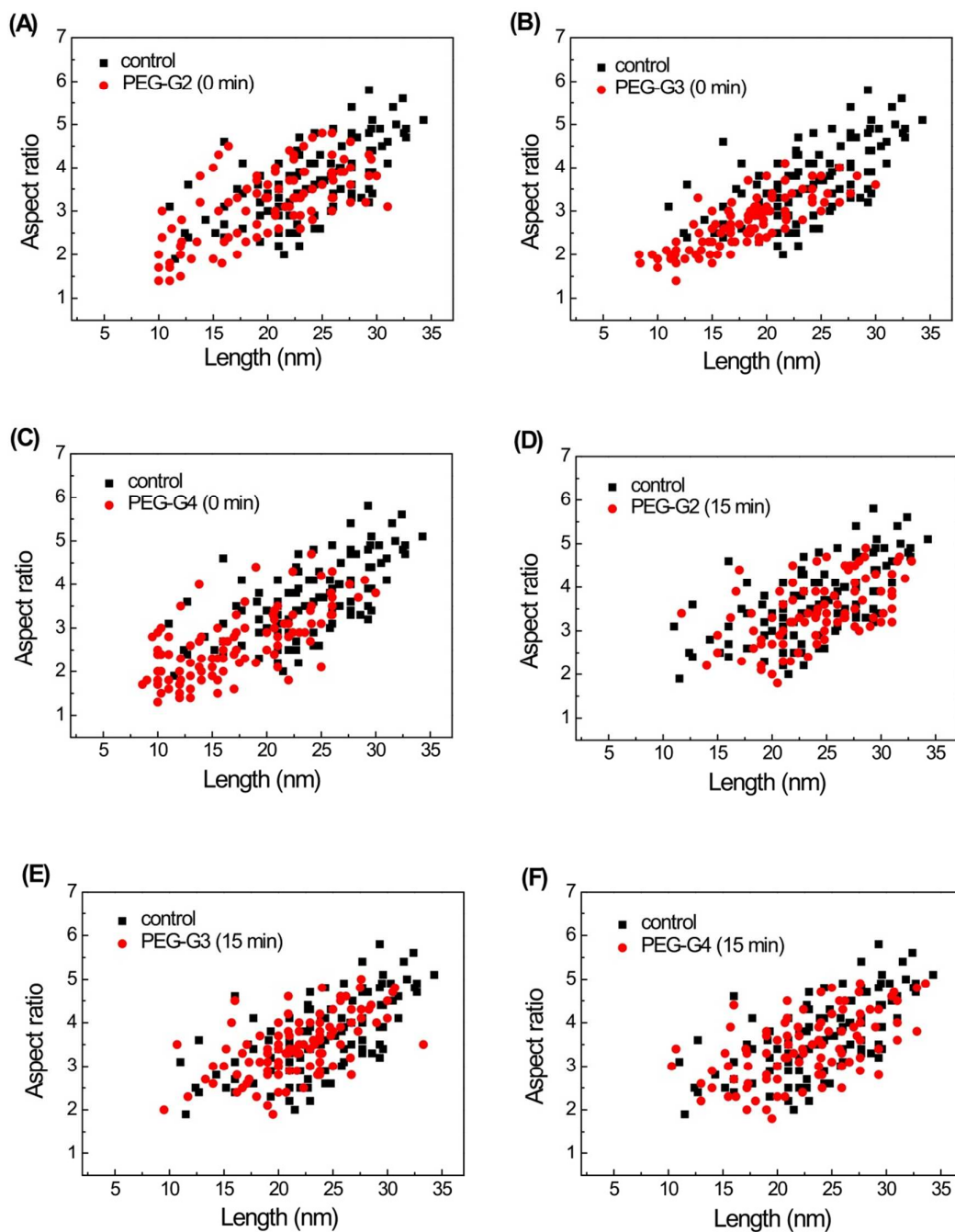


Figure 3. Relationship between length and aspect ratio for GNRs prepared with and PEG-cys-PAMAM G2 (A,D) G3 (B,E) and G4 (C,F) dendrimers without the delay time (A,B,C) or with the delay time of 15 min (D,E,F). Data for GNRs prepared without dendrimers are also given in each figure as a control.

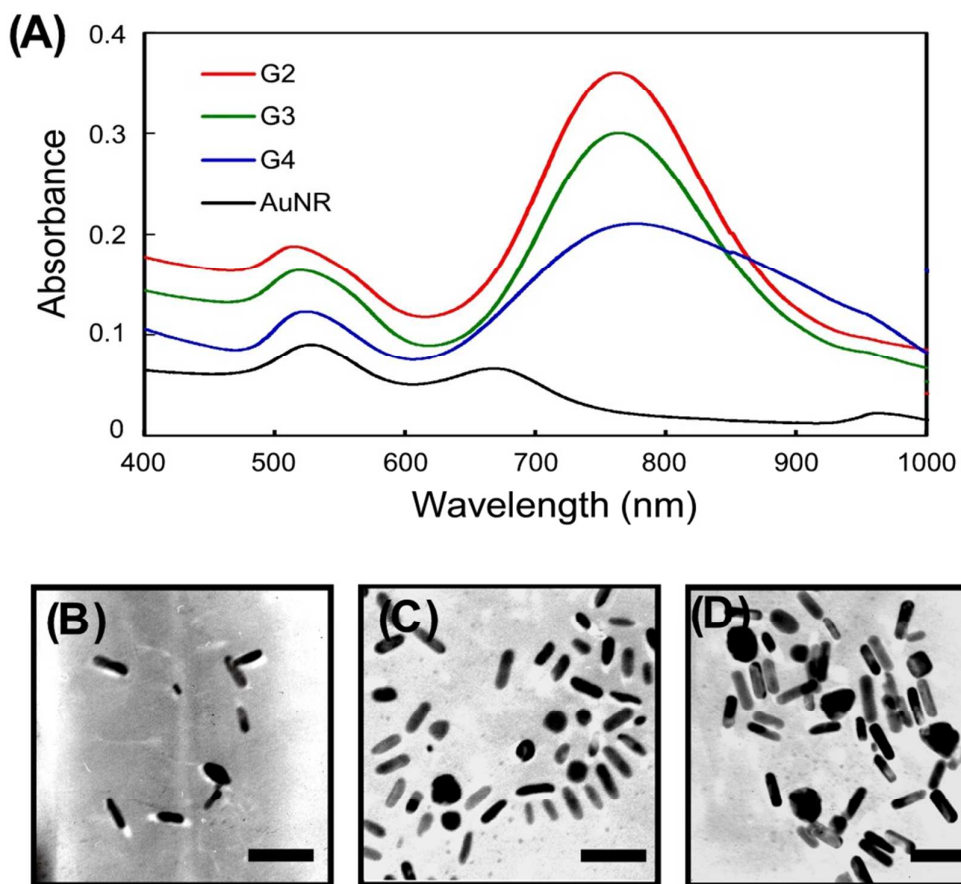


Figure 4. (A) Typical absorption spectra of PEG-PAMAM G2 dendron-attached GNRs, PEG-PAMAM G3 dendron-attached GNRs, PEG-PAMAM G4 dendron-attached GNRs, and GNRs without dendrons. TEM images of (B) PEG-PAMAM G2 dendron-attached GNRs, (C) PEG-PAMAM G3 dendron-attached GNRs, and (D) PEG-PAMAM G4 dendron-attached GNRs. Both absorption spectra and TEM images of GNRs were measured after 48 h incubation without or with dendrons, followed by two cycles of centrifugation. The scale bar in TEM images is 30 nm.

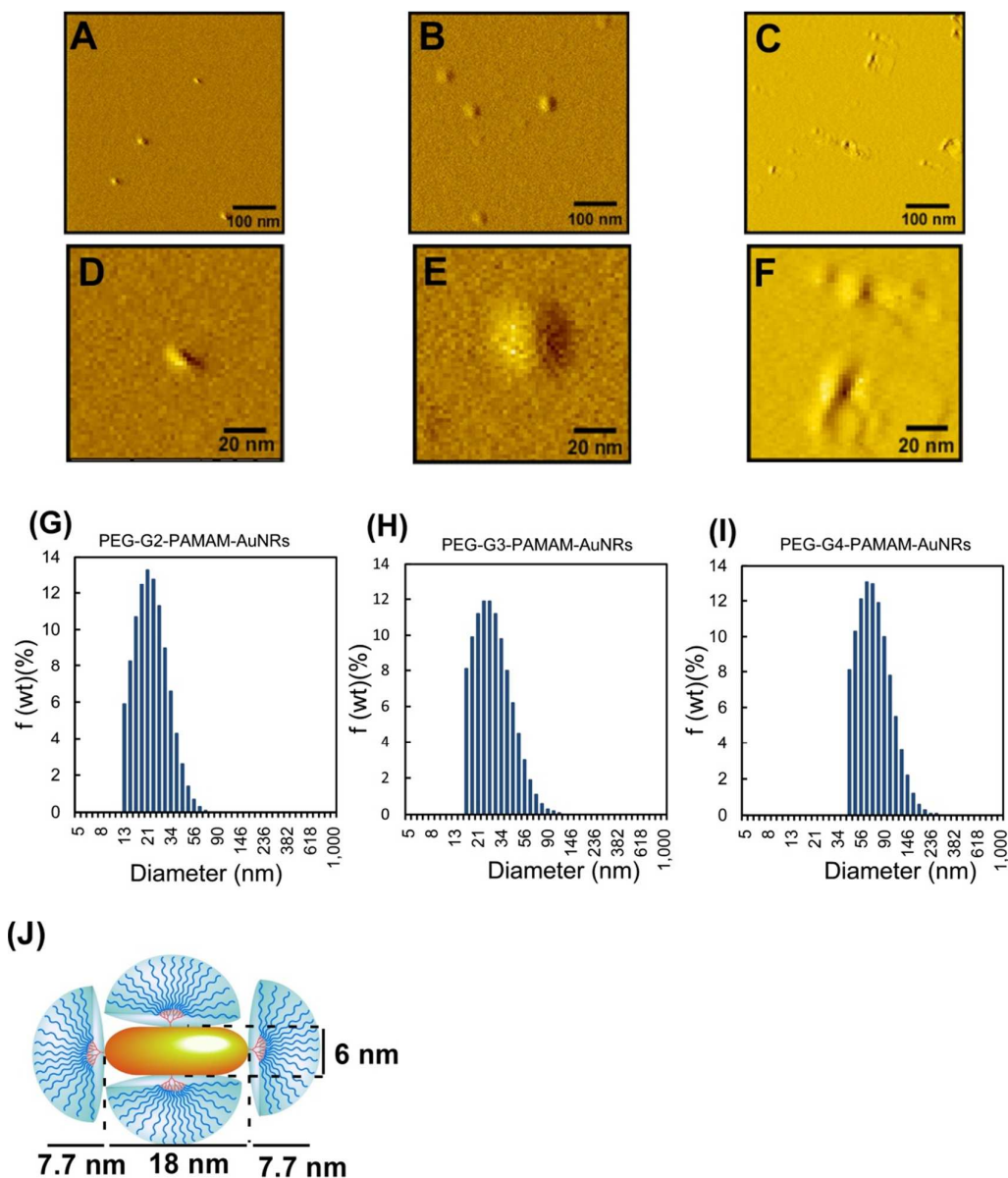


Figure 5. AFM images of PEG-PAMAM G2 (A, D), G3 (B, E), and G4 (C, F) dendron-attached GNRs. Size distributions of PEG-PAMAM G2 (G), G3 (H), and G4 (I) dendron-attached GNRs based on DLS measurements. (J) Schematic illustration of structure of PEG-PAMAM G3 dendron-attached GNR.



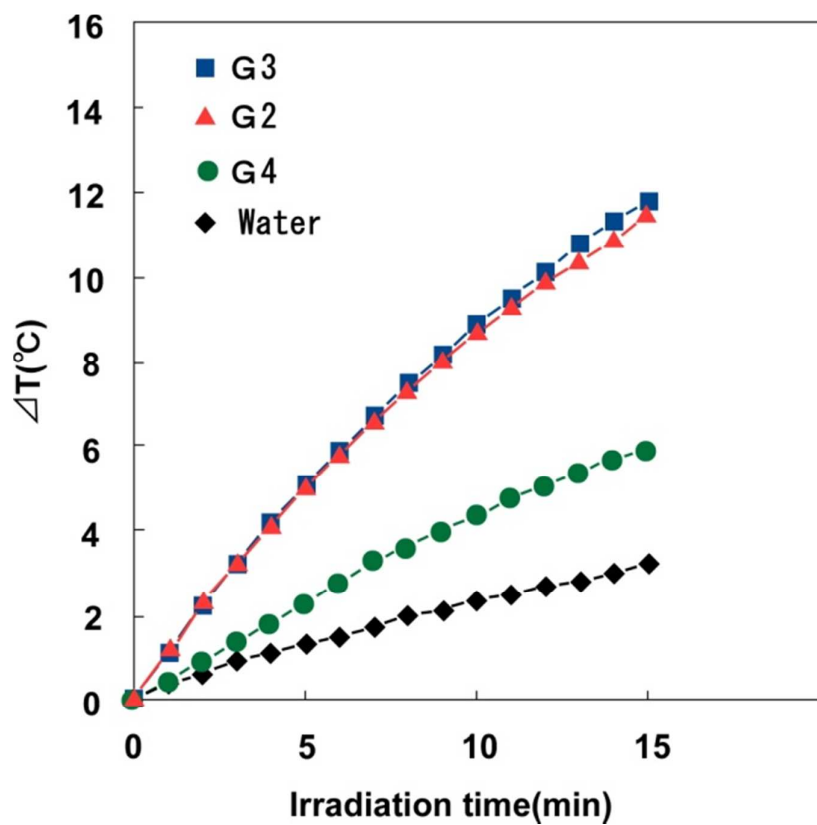


Figure 6. Temperature increment of water and aqueous PEG-PAMAM G2, G3 and G4 dendron-attached GNR solutions under 808 nm laser irradiation ( $6 \text{ W/cm}^2$ ). Initial temperature was  $24^\circ\text{C}$ . Au concentration was  $30 \mu\text{M}$ .

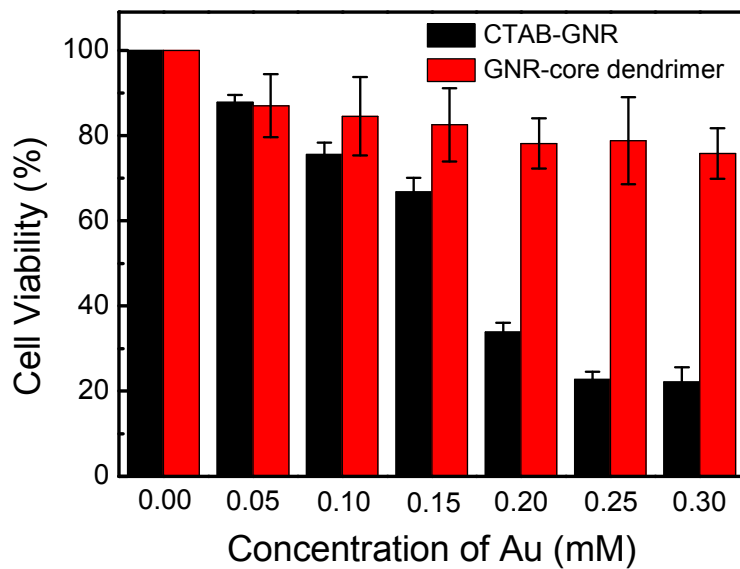


Figure 7. Cytotoxicity of unmodified GNR and GNR-core PEG-PAMAM G3 dendrimer to HeLa cells at different Au concentrations. Data are given as the mean  $\pm$  SD (n=3).

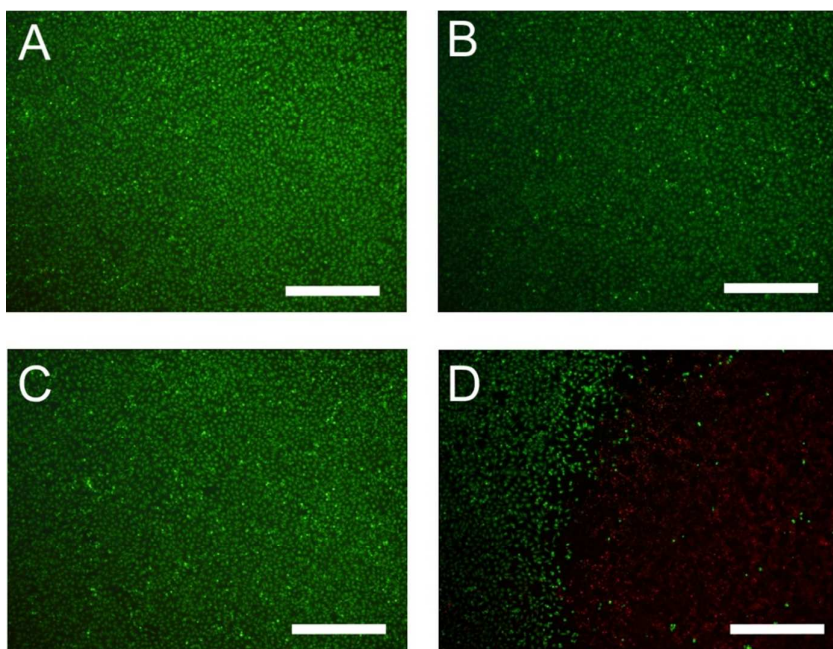


Figure 8. Fluorescence microscopic observation of NIR-induced cell-killing by GNR-core PEG-PAMAM G3 dendrimer. HeLa cells were treated with GNR-core PEG-PAMAM G3 dendrimer for 3 h at Au concentration of 0.25 mM, washed with PBS and irradiated with NIR laser ( $\lambda=808$  nm,  $6$  W/cm<sup>2</sup>) for 10 min. Cells without (A,C) and with (B,D) dendrimer treatment before (A,B) and after (C,D) NIR laser irradiation were stained with calcein-AM and propidium iodide and observed using a fluorescence microscope. The scale bar represents 1 mm. Calcein-AM fluorescence (green) and propidium iodide fluorescence (red) respectively show living and dead cells.

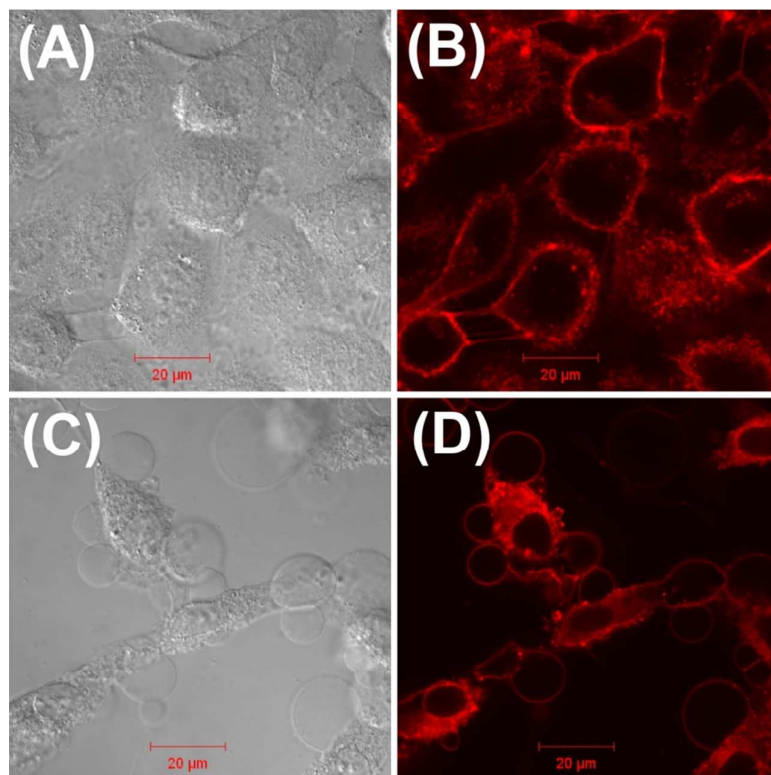


Figure 9. CLSM images of HeLa cells stained with Dil. HeLa cells were treated with GNR-core PEG-PAMAM G3 dendrimer for 3 h at Au concentration of 0.25 mM, washed with PBS, and observed immediately (A,B) or after NIR laser ( $\lambda=808$  nm, 6 W/cm<sup>2</sup>) irradiation for 10 min (C,D) using CLSM.

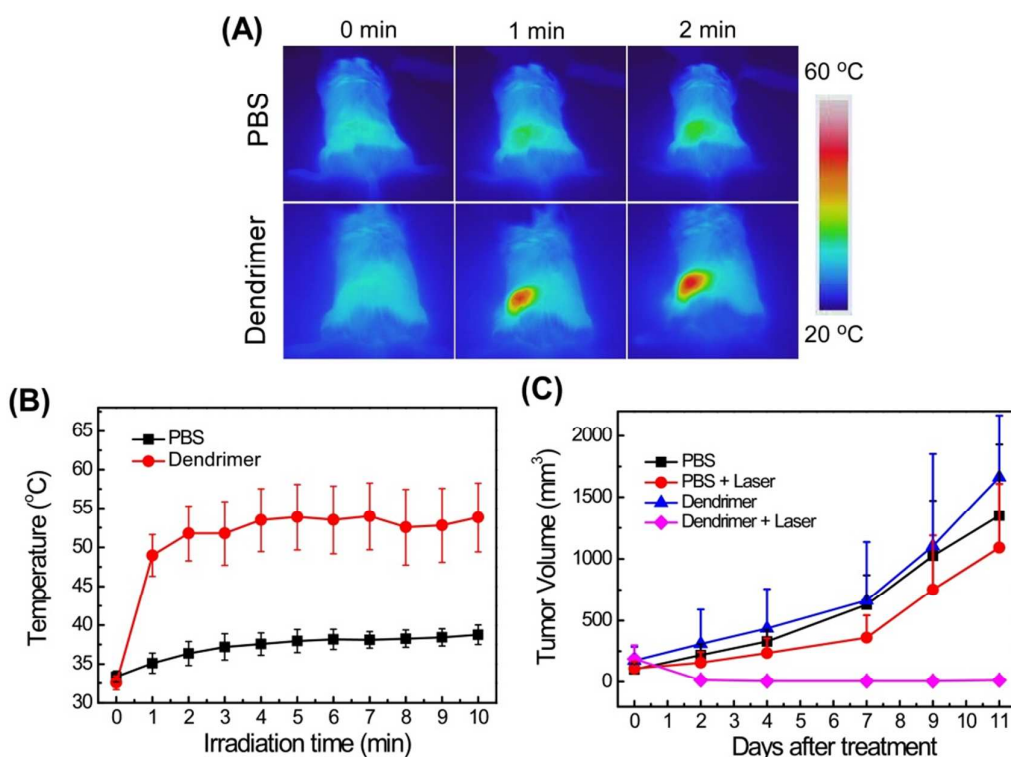
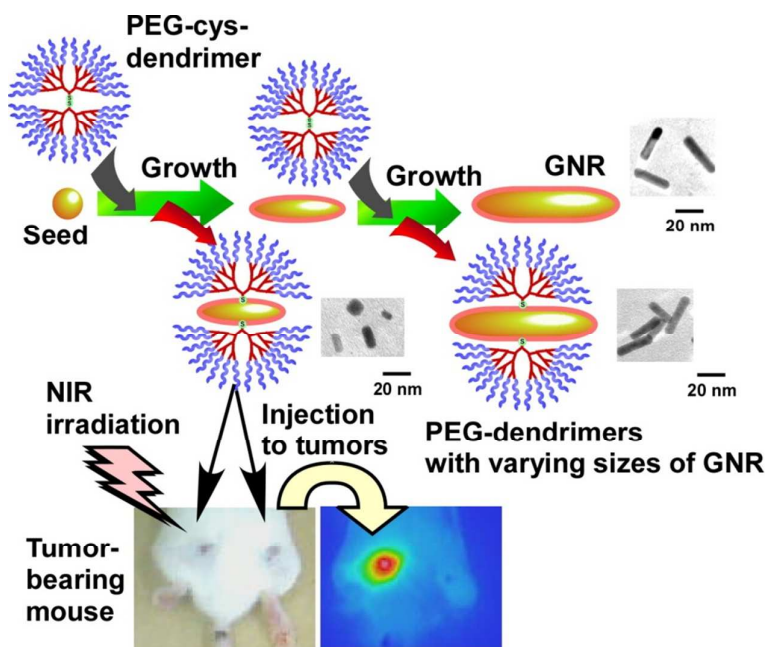


Figure 10. Photothermal effects of GNR-core PEG-PAMAM G3 dendrimer on tumor suppression for mice having colon carcinoma 26 tumors. Tumors were injected with GNR-core PEG-PAMAM G3 dendrimer or PBS and the left tumors were irradiated with NIR laser ( $\lambda=808$  nm,  $0.24$  W/cm<sup>2</sup>) for 10 min. (A) Thermographic images of tumors before and 1 min and 2 min after NIR laser irradiation. (B) Time courses of temperature of the left tumor injected with the dendrimer or PBS under NIR laser irradiation. (C) Time courses for volumes of tumors with various treatments. Six mice per group were used and data were given as mean  $\pm$  SD ( $n=6$ ) (B, C).



A new type of hybrid dendrimers consisting of a gold nanorod core and polyethylene glycol-modified polyamidoamine dendrons was developed for biomedical applications such as photothermal therapy.

Graphic for abstract